

Ultra Wideband Novel Printed Heptagonal Patch Antenna for Wireless Communication Applications

**Asst. Prof. Dr. Abdulkareem S. Abdullah, Lect. Malik J. Farhan
(Ph.D. Student)**

**Department of Electrical Engineering, College of Engineering,
University of Basrah, Basrah-IRAQ**

Emails: drasabdallah@ieee.org; malik_jf1974@yahoo.com

Abstract-

A novel printed heptagonal patch antenna is proposed in this paper to be used in the ultra wideband (UWB) applications. The proposed antenna consists of a heptagonal patch with appropriate dimensions on one side of a dielectric substrate, and a partial ground plane on the adverse side of the substrate. In order to cover the whole bandwidth allocated for UWB applications, many techniques are used in this paper to optimize the design of proposed antenna such as; adjusting the gap between the heptagonal patch and the ground plane, the feed position of the heptagonal patch, and the width and length of the ground plane under the heptagonal patch. The parameters of the proposed antenna such as the radiation pattern, gain, and impedance bandwidth are investigated and found be acceptable over the entire operational bandwidth. The proposed antenna also shows a good time domain characteristics and has a linear phase over this band giving less distortion of the received signal.

The program which is used in the design of the proposed antenna is High Frequency Structure Simulator (HFSS).

Index Terms: Heptagonal antenna, patch antenna, printed antenna (circuit) and UWB antenna.

هواني مبتكر للحزمة الفانقة ذو الرقعة السباعية المطبوعة لتطبيقات الاتصالات اللاسلكية

أ.م.د. عبد الكريم سوادي عبدالله ، م.مالك جاسم فرحان (طالب دكتوراه)

قسم الهندسة الكهربائية، كلية الهندسة، جامعة البصرة.

Emails: drasabdallah@ieee.org; malik_jf1974@yahoo.com

الخلاصة:

في هذا البحث تم تصميم هواني ذو رقعة مطبوعة سباعية الشكل والذى اقترح ليعمل في التطبيقات فانقة الحزمه التردديه. ان الهواني المقترن يتكون من رقعة سباعية الشكل بابعاد مناسبة تحفر على احدى جانبيه مرتكز العازل، اما في الجانب المقابل من مرتكز العازل فتحتوي على مستوى الارضي المجزئه. ولتغطية الحزمه الكامله المخصصة لتطبيقات فانقة الحزمه تم استخدام عدة تقنيات في هذا البحث للوصول الى التصميم المناسب للهواني المقترن وهذه التقنيات هي: تحديد الفجوة بين الرقعة السباعية ومستوى الارضي، تحديد نقطة التغذية المناسبة للرقعة السباعية، تحديد الطول والعرض المناسبين لمستوى الارضي.

ان خواص الاشعاع مثل نمط الاشعاع، الكسب و حزمه الممانعة للهواني المقترن تم فحصها وقد وجدت بانها مناسبة لحزمه العمل. وكذلك قد بين الهواني المقترن بانه يمتلك خصائص مجال وقت جيدة ويمتلك طور خطى على طول حزمه العمل وهذا يعني انه سوف يستقبل اشارات بتثنوية قليل.

1-INTRODUCTION

The ultra wideband (UWB) radio system has attracted both academic and industrial communities attentions since the Federal Communication Committee (FCC) approval of frequency band between 3.1 to 10.6 GHz for commercial applications in 2002 [1].

Finding a suitable antenna design for the implementation of UWB systems remains a challenge still. Planar antennas are good candidates for UWB radio system integration because of the merits of lightweight, low profile and cost effective [2-17]. Mainly, the printed antenna consists of the planar radiator and ground plane etched oppositely onto the dielectric substrate of the printed-circuit boards (PCBs). In some configurations, the ground plane may be coplanar with the radiators. The radiators can be fed by a microstrip line and coaxial cable [18].

In this paper, a printed heptagonal patch antenna is proposed to be used in UWB applications. The antenna consists of a heptagonal patch and a partial ground plane etched on opposite sides of the substrate. The radiator is fed through a 50Ω microstrip line. After setting up the configuration of the antenna, determining the initial parameters and fixing the lower frequency, a parametric study is performed to confirm the calculated parameters. Then several bandwidth enhancement techniques are applied to widen the bandwidth and obtain UWB performance. These techniques are: adjusting the gap between radiating element and ground plane technique, the partial ground technique, and optimum feed point technique.

2-ANTENNA DESIGN

The proposed radiator shape is selected to be heptagonal as shown in Figure 1 with the FR4 dielectric substrate, which has a relative permittivity $\epsilon_r = 4.4$ and a thickness $h = 1.5$ mm.

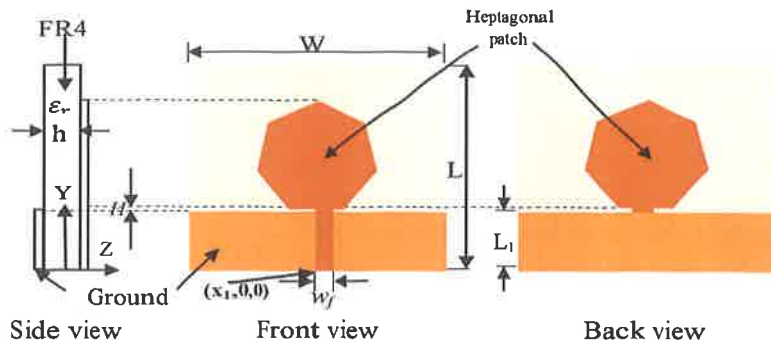


Figure 1: The proposed heptagonal Patch Antenna

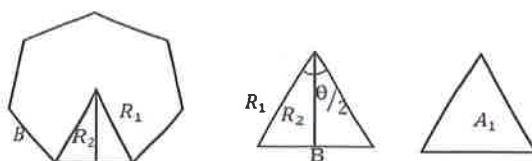


Figure 2: The geometry of the heptagonal Patch

$$R_2 = R_1 \cos(\theta/2) \approx 0.9R_1 \quad \dots (1)$$

where θ is equal to 51.428° . The area (A_1) of the triangular shown in Figure 2 is therefore equal to:

$$A_1 = \frac{1}{2}B \times R_2 = \frac{1}{2}B \times 0.9 \times R_1 = \frac{1}{2}0.7812 \times R_1^2 = 0.391 \times R_1^2$$

where $B \approx 0.868R_1$ approximately in heptagon. The total area of the heptagonal structure is then equal to:

$$A = 7 \times A_1 = 2.737R_1^2 \quad \dots (2)$$

In monopole antenna, it is found that the frequency corresponding to the lower edge of the bandwidth can be predicted approximately by equating the area of the plane configuration to that of cylindrical wire. The same principle can be applied on the proposed heptagonal structure, and therefore[19].

$$\} \quad 2\pi r l = 2.737 R_1^2 \quad \dots (3)$$

where:

r-the equivalent radius of the cylindrical wire.

l-the height of the cylindrical wire.

R₁-the main radius of the heptagonal patch.

The resonant frequency (**f_L**), which corresponds to the lower edge of the bandwidth is given by [19]:

$$f_L(\text{GHz}) = \frac{30 \times 0.24}{(l + r)}$$

$$\text{or} \quad f_L(\text{GHz}) = \frac{c}{\lambda} = \frac{7.2}{(R_1 + 0.4356R_1)} \quad \dots (4)$$

The dimensions of **l**, **r**, **R₁** are all in centimeters.

In order to include the effect of substrate, equation (4) should be modified as:

$$f_L(\text{GHz}) = \frac{7.2}{(R_1 + 0.4356R_1)\sqrt{\epsilon_{\text{eff}}}} \quad \dots (5)$$

where **ε_{eff}** represents the effective relative permittivity of the dielectric substrate, and given by [20]

$$\epsilon_{\text{eff}} \approx \frac{\epsilon_r + 1}{2} \quad \dots (6)$$

The width (w_f) of the microstrip feed line is calculated according to the following equation. [20]

$$Z_c = \frac{120\pi}{\sqrt{\epsilon_{\text{eff}}}\left[\frac{w_f}{h} + 1.393 + 0.667\ln\left(\frac{w_f}{h} + 1.444\right)\right]} \quad \dots (7)$$

where Z_c is the characteristic impedance

1. ANTENNA PARAMETRIC STUDY

The main radius (R_1) of the heptagon is calculated according to Equation 5 as (0.9847cm), and therefore (B) and (R_2) are found as (0.8545cm) and (0.8871cm) respectively.

The heptagonal patch with a radius (R_1) and a 50Ω microstrip feed line are printed on one side of the FR4 substrate. The length and width of the substrate are denoted by (L) and (W) respectively. The width (w_f) of the microstrip feed line is calculated as 2.89mm according to equation (7) in order to achieve 50Ω characteristic impedance. The ground plane is etched on the other side of the substrate and has a length of (L_1), which actually covers, a section of the feeder line. The feed gap between the feed point and the ground plane is denoted by (H). The feed point position of the patch edge is denoted by (x_1) as depicted in Figure 1.

The antenna performance is mainly affected by the geometrical and electrical parameters, such as the dimensions of the ground plane, feed gap size, feed point position and relation between the widths of ground plane and patch. In this section, the important parameters that affect the antenna performance will be analyzed and a parametric study is carried out to optimize the antenna performance.

3.1-Feed Gap (H)

The first parameter to be optimized is the feed gap (H). The optimization process is done by considering $R_1=9.847\text{mm}$, the dimensions of the ground plane are arbitrary selected as $L_1=14\text{mm}$ and $W=20\text{mm}$ just to cover the patch width and partially the feed line length. It is found that the response at these dimensions will give bandwidth that covers the whole frequency range according to FCC(3.1-10.6GHz).

The simulated return loss with respect to frequency is shown in Figure 3 for different values of feed gap (H). It is clear that the changing of (H) parameter has a significant influence on the -10dB bandwidth. Actually, this bandwidth becomes narrower as (H) becomes larger since the impedance matching of the antenna becomes worse. It is also noticed that the lower resonant frequency is not affected by the increasing of (H), while the higher resonant frequency is apparently affected by the increasing of (H). thus the optimum feed position is found to be at a feed gap of $H=0.7\text{mm}$, at this value, the real part of the antenna input impedance shown in Figure 4 varies slowly around the 50Ω value, while the imaginary part of the antenna input impedance remains small across a wide frequency range, leading to a UWB performance. Table 1 summarizes the values of the lower and upper resonant frequencies along with their respective bandwidths.

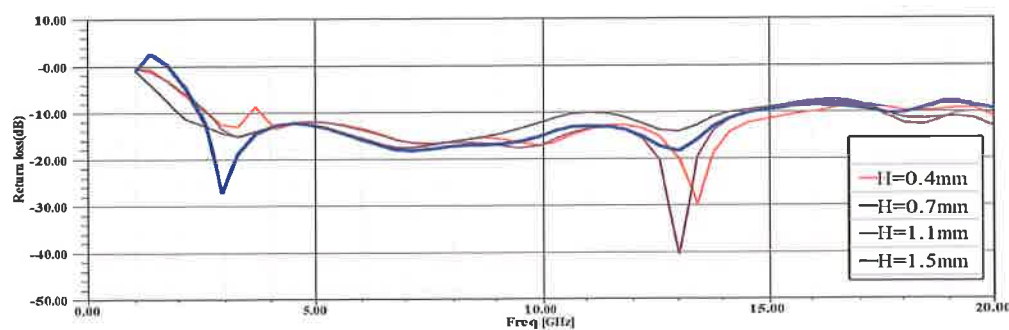


Figure 3: Simulated return loss of heptagonal patch antenna for different feed gaps with $R_1=9.847\text{mm}$, $L_1=14\text{mm}$ and $W=20\text{mm}$

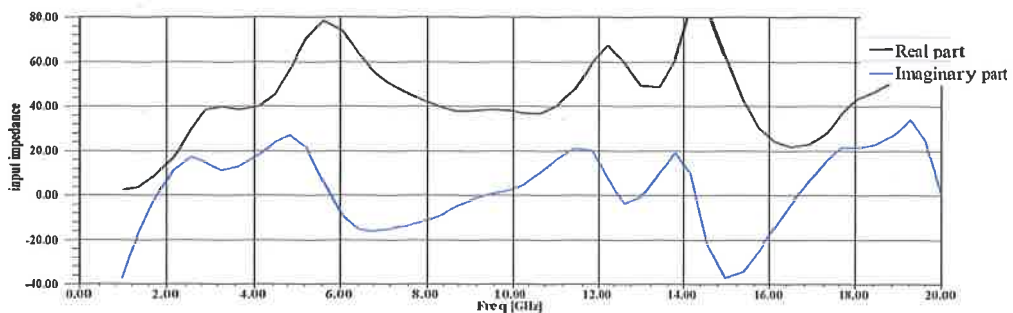


Figure 4: Simulated input impedance of heptagonal patch antenna for feed gap of $H = 0.7\text{mm}$ with $R_1 = 9.847\text{mm}$, $L_1 = 14\text{mm}$ and $W = 20\text{mm}$

Table1: Feed gap distance (H) against the bandwidth of heptagonal patch antenna

H(m m)	Lower resonant frequency(GHz)	Upper resonant frequency(GHz)	Bandwidth (GHz)
0.4	3.83	16	12.17
0.7	2.58	14.8	12.22
1.1	2.43	14.5	12.07
1.5	2	11.2	9.2

3.2 -Feed Point Position (x_1)

The second parameter to be optimized is the feed point position (x_1). The value of H is taken as the optimized value of 0.7mm, while the values of R_1 , L_1 , and W are kept as same as in the previous. Figure 5 shows the simulation return loss of the antenna with respect to frequency. It is shown that the impedance matching is getting worse as (x_1) becomes very close to any patch side. It is clear that as the feed point becomes near the patch center, the impedance matching of antenna increases, and consequently a larger bandwidth is obtained. This is due to the symmetry of current distribution along the patch.

The values of feed point position range is taken from the left side to right side of the lower edge of heptagonal patch and the optimal value is found at $x_1=19.478\text{mm}$. The peak values of the real part and imaginary part of the antenna are found to be 85Ω and 28Ω respectively as shown in Figure 6. It is noticed that, at the frequencies where the real part is close to 50Ω , the imaginary part is close to zero. As a result, the antenna input impedance is matched well to the 50Ω feeder, leading a wide operating bandwidth. Table 2 summarizes the values of the lower and upper resonant frequencies along with their respective bandwidths.

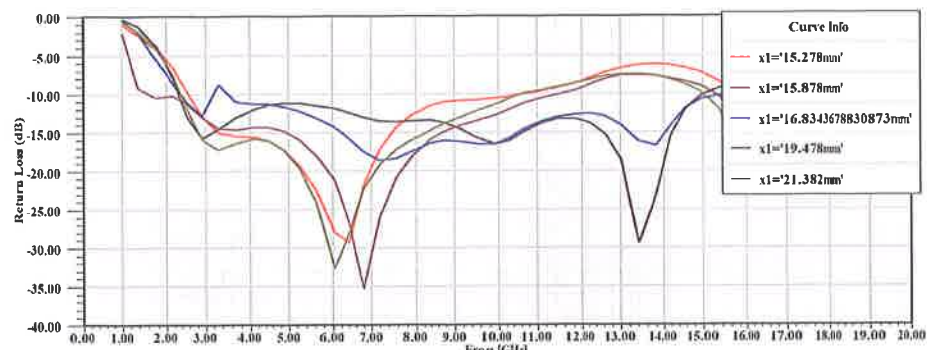


Figure 5: Simulated return loss of heptagonal patch antenna for different feed point positions with $R_1= 9.847\text{mm}$, $L_1= 14\text{mm}$, $H=0.7\text{mm}$ and $W=20\text{mm}$

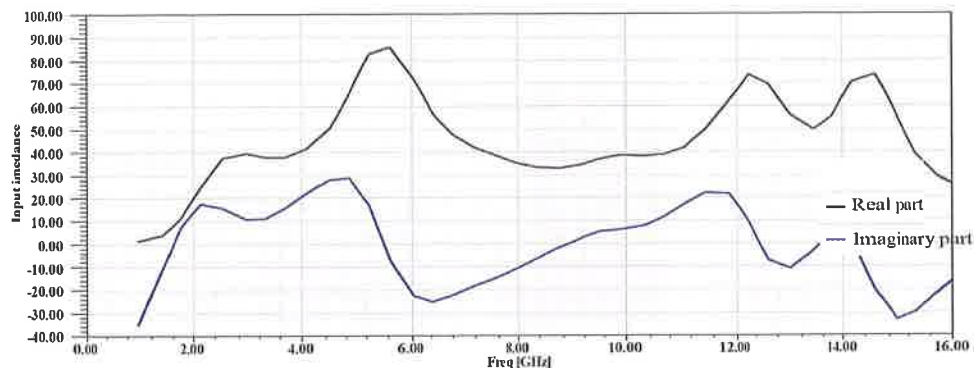


Figure 6: Simulated input impedance of heptagonal patch antenna for feed point position $x_1=19.478\text{mm}$ with $R_1= 9.847\text{mm}$, $L_1= 14\text{mm}$, $H=0.7\text{mm}$ and $W=20\text{mm}$

Table 2: Feed point position (x_1) against the bandwidth of heptagonal patch antenna

x_1 (mm)	Lower resonant frequency (GHz)	Upper resonant frequency (GHz)	Bandwidth (GHz)
15.278	2.6	10.78	8.18
15.878	1.62	11.5	9.88
16.834	3.55	17.3	13.75
19.478	2.3	15.1	12.8
21.382	2.38	10.65	8.27

3.3-Ground Plane Width (W)

The third parameter to be optimized is the ground plane width (W) using $R_1=9.847\text{mm}$, $L_1=14\text{mm}$, $H=0.7\text{mm}$ and $x_1=19.478\text{mm}$. Figure 7 shows the simulated antenna return loss for different values of the ground plane width (W). The influence of the ground plane width variation is clear through shifting all the resonance modes across the spectrum. It is noticeable that the -10dB bandwidth is reduced when the ground plane width is either too wide or too narrow. According to the Figure 7 the best response over the entire frequency range is found at $W=40\text{mm}$ therefore, this value is taken as optimal value of ground plane width. Actually, when the ground plane width is either increased or decreased from its optimal value, the current distribution on the top edge of the ground plane is also changed. This phenomenon is happened due to an increase or decrease of the antenna inductance if it is treated as a resonating circuit, causing the position change of the first resonance mode in the spectrum. It also causes the frequencies of the higher modes to be unevenly shifted.

Table 3 summarizes the values of the lower and upper resonant frequencies along with their respective bandwidths.

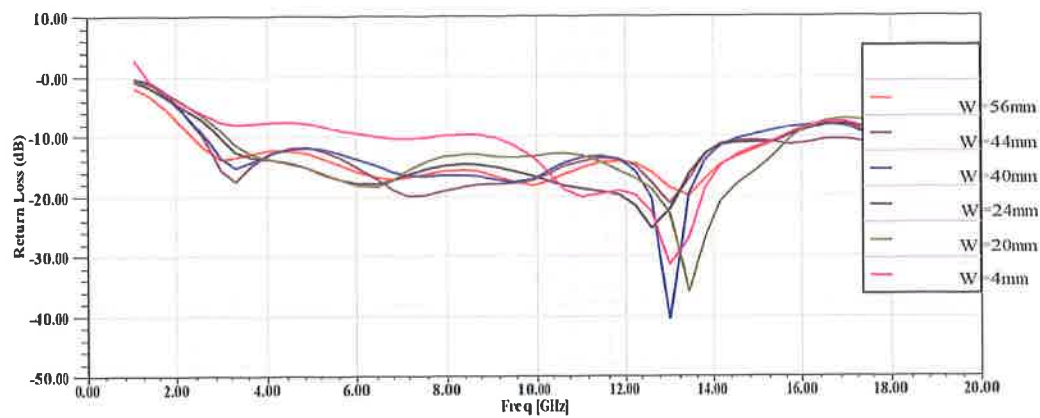


Figure 7: Simulated return loss of heptagonal patch antenna for different ground widths with feed point position $x_1=19.478\text{mm}$, $R_1=9.847\text{mm}$, $H=0.7\text{mm}$ and

Table 3: Ground plane width (W) against the bandwidth of heptagonal patch antenna

W(m m)	Lower resonant frequency (GHz)	Upper resonant frequency (GHz)	Bandwidth (GHz)
56	2.35	15.6	13.25
44	2.55	18.7	16.15
40	2.6	14.96	12.36
24	2.9	15.75	12.85
20	3.1	15.8	12.7
4	6.3	7.9	1.6

3.4-Ground Plane Length (L_1)

The fourth parameter to be optimized is the ground plane length (L_1) using $R_1=9.847\text{mm}$, $W=40\text{mm}$, $H=0.7\text{mm}$ and $x_1=19.478\text{mm}$. The

simulated antenna return loss as (L_1) is changed from 5mm to 19mm is shown in Figure 8. It is obvious that the antenna -10dB bandwidth does not change much with the variation of (L_1). Since the current of the antenna is mainly distributed along the y-direction, therefore, the antenna input impedance and, hence the bandwidth, is mainly determined by its width (W). The ground plane length (L_1) can be reduced significantly without any sacrifice of the bandwidth, leading to a procedure for miniaturization of antenna size. Table 4 summarizes the values of lower and upper resonant frequencies along with their respective bandwidths.

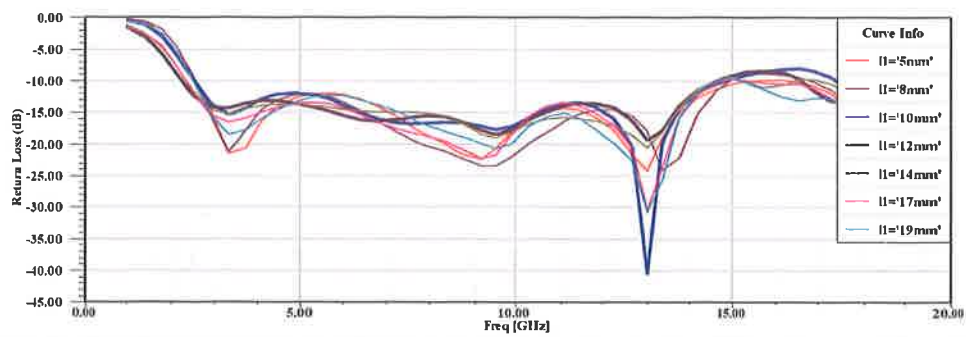


Figure 8: Simulated return loss of heptagonal patch antenna for different ground lengths with feed point position $x_1=19.478\text{mm}$, $R_1=9.847\text{mm}$, $W=40\text{mm}$ and $H=0.7\text{mm}$

Table 4: The -10dB bandwidths for different lengths of the ground plane L_1

$L_1(\text{mm})$	Lower resonant frequency (GHz)	Upper resonant frequency (GHz)	Bandwidth (GHz)
5	2.62	15.45	12.83
8	2.61	14.96	12.35
10	2.59	14.8	12.21
12	2.257	14.6	12.343
14	2.359	14.54	12.181
17	2.357	14.8	12.443
19	2.552	14.54	11.988

3.5-Length of substrate (L)

The fifth parameter to be optimized is the length of substrate (L) using $R_1=9.847\text{mm}$, $W=40\text{mm}$, $H=0.7\text{mm}$, $x_1=19.478\text{mm}$ and $L_1=10\text{mm}$. The simulated return loss versus the frequency for different values of the length of the substrate (L) is presented in Figure 9. It is clear that the bandwidth of proposed antenna does not change very much with the variation of (L). Therefore, the substrate length (L) can be taken just to cover the microstrip line length, feed gap distance (H) and the distance from the lower edge of the patch to its tip. The optimal value of substrate length (L) is found to be at $L=32\text{mm}$.

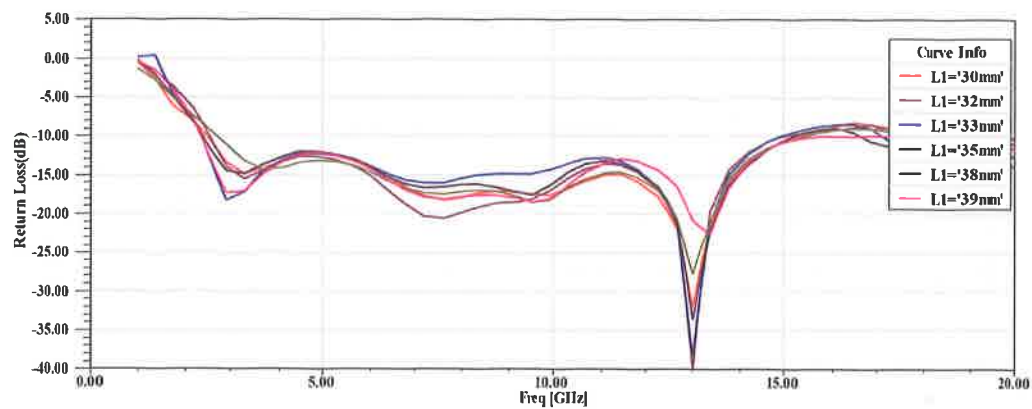


Figure 9: Simulated return loss of heptagonal patch antenna for different substrate lengths with $x_1=19.478\text{mm}$, $R_1=9.847\text{mm}$, $W=40\text{mm}$, $L_1=10\text{mm}$ and $H=0.7\text{mm}$

4-THE OPTIMIZED DESIGN

The optimized heptagonal patch antenna is constructed as shown in Figure 10 taking into account the final parameter values as shown in Table 5.

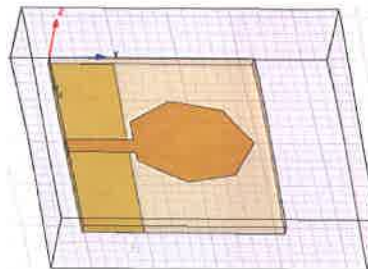


Figure 10: The prototype of the heptagonal patch antenna with $x_1=19.478\text{mm}$, $R_1=9.847\text{mm}$, $L_1=10\text{mm}$, $W=40\text{mm}$, $H=0.7\text{mm}$ and $L=32\text{mm}$

Table 5: Optimal design parameters of heptagonal patch antenna

Parameter	Value
substrate thickness (h)	1.5mm
relative permittivity (ϵ_r)	4.4
length of the substrate (L)	32mm
width of the substrate (W)	40mm
width of the microstrip feed line (W_f)	2.89mm
ground plane length (L_1)	10mm
feed gap (H)	0.7mm
feed point position (x_1)	19.478mm

5-RESULTS AND DISCUSSION

The optimized antenna structure with a prescribed parameter value mentioned in Table 5 is first simulated at three different frequencies 3.5GHz, 7.5 GHz and 13.5 GHz, and the resulted current distributions at these frequencies are presented in Figure 11.

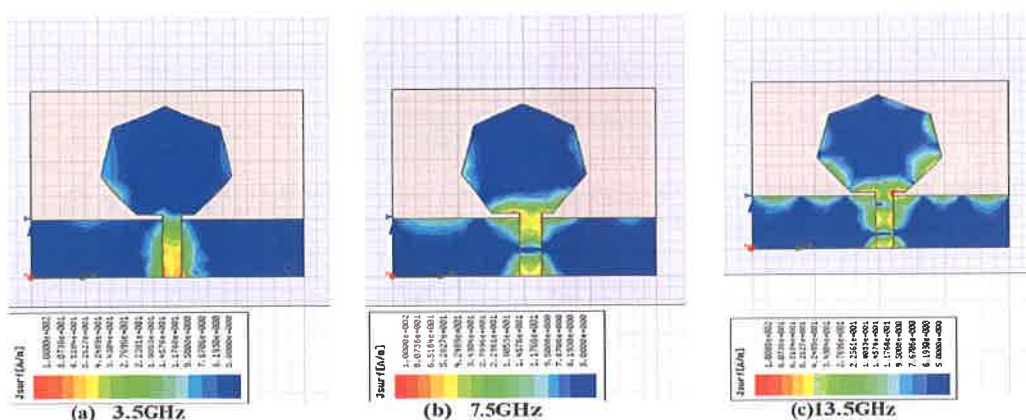


Figure 11: Simulated current distribution of the optimized heptagonal patch antenna for different resonance frequencies with the strength of current distribution ranges

It is clear that, for the three different frequencies, the current distribution is mainly concentrated along the lower edge of the patch. This may explain why the first resonant frequency is affected by the patch dimension. On the other hand, the current distribution on the ground plane is concentrated along the y-direction within a narrow area. This is due to the fact that the antenna performance is dependent on the ground plane width (W) rather than its length (L).

5.1-Return Loss

The return loss of optimized antenna structure is shown in Figure 12. The -10dB bandwidth is found to be approximately more than 12GHz. It is clear that the optimized antenna can support multiple closely distributed resonance modes. Actually, the UWB characteristic of this antenna is attributed to the overlapping of these resonance modes.

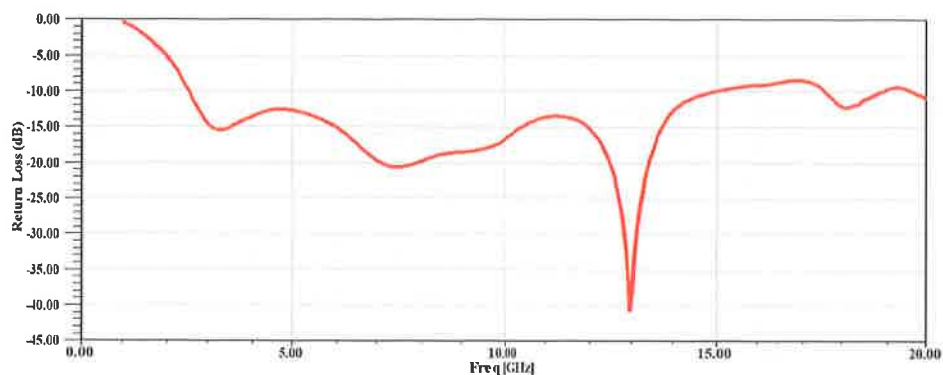


Figure 12: simulated return loss of the heptagonal patch antenna with optimum dimensions

5.2-Radiation Patterns

The E-plane and H-plane radiation patterns of the optimized antenna structure are shown in Figures 13, 14 and 15 at frequencies 3.5 GHz, 7.5 GHz and 13.5 GHz respectively. The radiation patterns for different frequencies show that the proposed antenna has omni-directional patterns (one of UWB properties) in the H-plane, and for the E-plane, at low frequencies form figure-of-eight patterns but at high frequencies, there are dips, the proposed antenna shows an acceptable radiation pattern in its whole operational bandwidth since the degradation happens only for a small part of the entire frequency range and it is not too drastic.

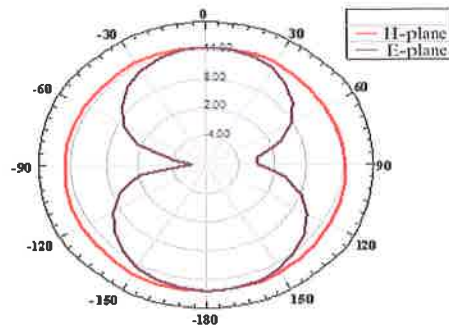


Figure 13: The simulated H-plane and E-plane radiation pattern at 3.5GHz

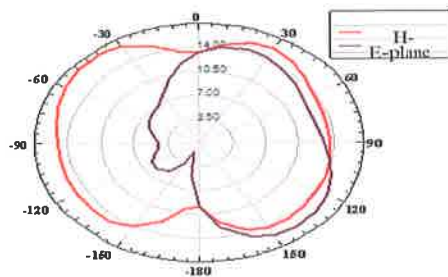


Figure 14: The simulated H-plane and E-plane radiation pattern at

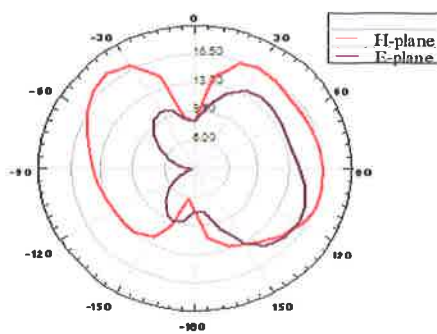


Figure 15: The simulated H-plane and E-plane radiation pattern at 13.5GHz

5.3-Antenna Gain

The simulated antenna gain versus frequency is shown in Figure 16, and found to be suitable for the UWB communications and applications.

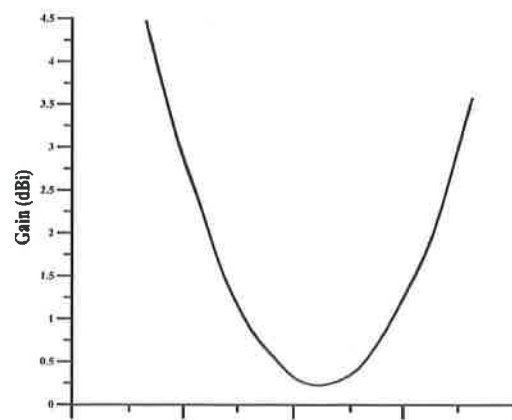


Figure 16: Gain of the heptagonal patch antenna for different frequencies

6-TIME DOMAIN PERFORMANCE OF THE OPTIMIZED ANTENNA

A good time domain performance is an essential issue in UWB antenna. Usually the received signals do not resemble the transmitted ones because of the distortions. To avoid the distortions in the received

signals, transfer function should have an approximate flat magnitude and linear phase response over the operational bandwidth. Group delay is usually used to evaluate the phase response, and ideally when group delay is constant the phase response is linear. To find the transfer function, a system set-up is used, as shown in Figure 17, which is comprised of two identical heptagonal patch antennas at the transmitter and receiver. The transmitted and received antennas are vertically placed with a separation of more than 20cm, which is consistent with the far field distance of all wave lengths in the frequency range ($d = 2D^2/\lambda$)[21].

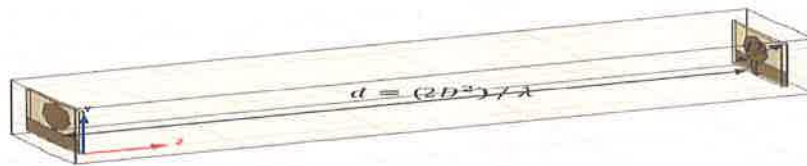


Figure 17: System set-up for calculating the antenna transfer function

6.1-Magnitude of Transfer Function

The magnitude of the transfer function of the heptagonal patch antenna pair is shown in Figure 18. The operating band corresponding to -10dB below the peak is less than 5.5GHz, which means that the signal within this band will be almost equally received. In the band 5.5 GHz-9.5 GHz, the magnitude of the transfer function decreases

sharply resulting in a distortion of the received signal. At frequencies higher than 9.5 GHz, the frequency components can be received without problems.

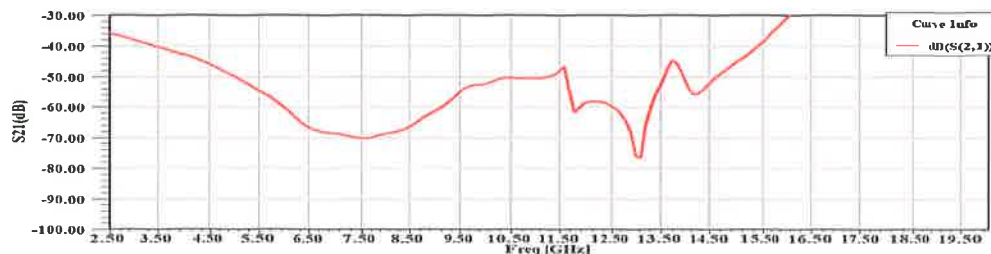


Figure 18: Magnitude of transfer function of heptagonal patch antennas pair

6,1-Phase of Transfer Function

The phase of the transfer function of the heptagonal patch antenna pair is shown in Figure 19. It is shown that this response is nearly linear over the band 1GHz to 12 GHz

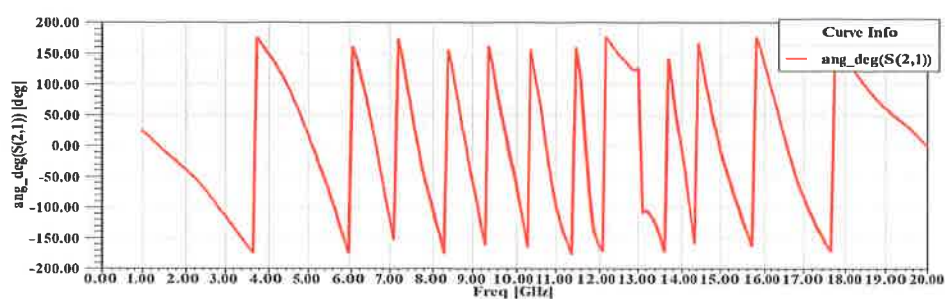


Figure 19: Phase of transfer function of heptagonal patch antenna pair

6,2-Group Delay of Transfer Function

The group delay of the transfer function of the heptagonal patch antenna pair is shown in Figure 20. This curve can be considered stable with variation less than 1.4ns in the band 1GHz to 11.8 GHz.

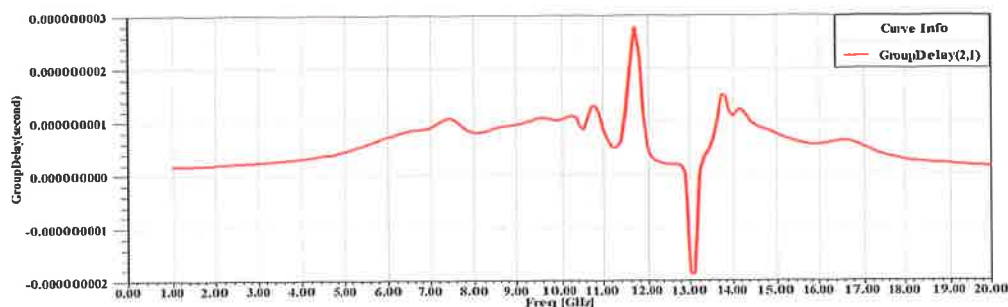


Figure 20: Group delay of transfer function of heptagonal patch antenna pair

7-CONCLUSION

A novel, small low-profile printed heptagonal patch antenna is designed and analyzed satisfy UWB requirements. The proposed antenna consists of a heptagonal patch and a partial ground plane etched on the opposite sides of a dielectric substrate and fed by a 50Ω microstrip line. The frequency domain characteristics of the antenna such as the radiation pattern, gain and impedance bandwidth are found acceptable in the entire operational frequency range. The time domain characteristics of the antenna also found acceptable, and the antenna proved to posses linear phase over the operational bandwidth, which leads to constant group delay and less distortion for the received signal.

REFERENCES

1. **First Report and Order, Revision of Part 15 of the Commission's Rules Regarding Ultra-wideband Transmission Systems** Federal Communication Commission, 02-48, April 22, 2002.
2. **Li, P. C., J. X. Liang, and X. D. Chen,** "Study of printed elliptical/circular slot antennas for ultra-wide band applications," **IEEE Transactions on Antennas and Propagation**, Vol.54, No.6, 1670-1675, 2006.
3. **Chen, Z. N., T. S. P. See, and X. M. Qing,** "Small printed ultra wideband antenna with reduced ground plane effect," **IEEE Trans. Antennas Propag.**, Vol.55, No.2, 383-388, 2007.
4. **Ray, K. P., and Y. Ranga,** "Ultrawideband printed elliptical monopole antennas," **IEEE Trans. Antennas Propag.**, Vol. 55, No. 4, 1189-1192, 2007.
5. **Sadat, S., M. Fardis, F. G. Gharakhili, and G. R. Dadashzadeh,** "A compact microstrip square-ring slot antenna for UWB applications," **Progress In Electromagnetics Research**, Vol.67, 173-179, 2007.
6. **Abbosh, A. M., and M. E. Bialkowski,** "Design of ultra wideband planar monopole antennas of circular and elliptical shape," **IEEE Trans. Antennas Propag.**, Vol.56, No.1, 17-23, 2008.
7. **Fallahi, R., A. A. Kalteh, and M. G. Roozbahani,** "A novel UWB elliptical slot antenna with band-notched characteristics," **Progress In Electromagnetics Research**, Vol.82, 127-136, 2008.
8. **Deng, J. Y., Y. Z. Yin, Q. Wang, and Q. Z. Liu,** "Study on a CPW-Fed UWB Antenna with Dual Band-Notched Characteristics", **Journal of Electromagnetic Waves and Applications**, Vol.23, 513-521, 2009.

9. Wang, H., H. Zhang, X. Liu, and K. Huang, "A CPW-FED ultra-wideband planar inverted cone antenna," *progress in Electromagnetics Research C*, Vol. 12, 101-112, 2010.
10. Abdollahvand, M., G. Dadashzadeh, and D. Mostafa, "Compact dual band-notched printed monopole antenna for UWB application," *IEEE Antennas and Wireless Propagation Letters*, Vol.9, 1148-1151, 2010.
11. Barbarino, S., and F. Consoli, "UWB circular slot antennawith an inverted-L notch filter for the 5 GHz WLAN band," *Progress In Electromagnetics Research*, Vol. 104, 1-13, 2010.
12. Kumar, M., A. Basu, and S. K. Koul, "UWB printed slot antenna with improved performance in time and frequency domains," *Progress In Electromagnetics Research C*, Vol. 18, 197-210, 2011.
13. Liao, X. J., H. C. Yang, N. Han, and Y. Li, "Aperture UWB antenna with triple band-notched characteristics," *Electronics Letters*, Vol. 47, No. 2, 2011.
14. Ghaderi, M. R., and F. Mohajeri, "A compact hexagonal wide slot antennas with microstrip fed monopole for UWB applications," *IEEE Antenna and Wireless Propagation Letter*, Vol. 10, 682-685, 2011.
15. Raghavan, S., Ch. Anandkumar, A. Subbarao, M. Ramaraj, and R. Pandeeswari, "A Compact Ultra Wideband EBG Antenna with Band Notched Characteristics," *Progress In Electromagnetics Research Symposium Proceedings*, Moscow, Russia, August 19-23, 2012.
16. Kasi, B., and C. K. Chakrabarty, "Ultra-wideband antenna array design for target detection, " *Progress In Electromagnetics Research C*, Vol.25, 67-79, 2012.

17. Mandal, T., and S. Das, "acoplanar waveguide fed ultra wideband hexagonal slot antenna with dual band rejection," *Progress In Electromagnetics Research C*, Vol.39, 209-224, 2013.
18. Chen, Z., N., M. J.Ammann, X. Qing X.,Hui Wu, X. Terence S.P. See, and A. Cai, "Planar Antennas," *IEEE Microwave Magazine*, Vol.7, No.1, 63-73, 2006.
19. Agrawall, N., Kumar, G. & Ray, K., "Wide-Band Planar Monopole Antennas, " *IEEE Transactions on Antennas and Propagation*, Vol. 46, No.2, 998, 294-295, 1998.
20. Liu, J. S. Gong, Y. Xu, X. Zhang,C. Feng,N. Qi, "Compact printed ultra wideband monopole antenna with dual band-notced characteristics," *Electronics Letters*, Vol.44, No.12, 710-711, 2008.
21. Balanis,C., A., "Antenna Theory Analysis and Design,"3rd ed.,JohnWiley& Sons, Inc., 2005.